Heliyon 10 (2024) e39445

Contents lists available at ScienceDirect

Heliyon

journal homepage: www.cell.com/heliyon

Research article

Validation of 2D lateral cephalometric analysis using artificial intelligence-processed low-dose cone beam computed tomography

Eun-Ji Chung [a,1], Byoung-Eun Yang [b,c,d,e,1], Sam-Hee Kang [a], Young-Hee Kim [d,f], Ji-Yeon Na [d,e,f], Sang-Yoon Park [b,c,d,e], Sung-Woon On [c,d,g], Soo-Hwan Byun [b,c,d,e,*]

[a] Department of Conservative Dentistry, Hallym University Sacred Heart Hospital, Anyang, 14066, Republic of Korea
[b] Department of Oral and Maxillofacial Surgery, Hallym University Sacred Heart Hospital, Anyang, 14066, Republic of Korea
[c] Graduate School of Clinical Dentistry, Hallym University, Chuncheon, 24252, Republic of Korea
[d] Institute of Clinical Dentistry, Hallym University, Chuncheon, 24252, Republic of Korea
[e] Dental AI-Robotics Center, Hallym University Sacred Heart Hospital, Anyang, 14066, Republic of Korea
[f] Department of Oral and Maxillofacial Radiology, Hallym University Sacred Heart Hospital, Anyang, 14066, Republic of Korea
[g] Department of Oral and Maxillofacial Surgery, Hallym University Dongtan Sacred Heart Hospital, Hwaseong, 18450, Republic of Korea

ARTICLE INFO

Keywords:
Cephalometric analysis
Cone beam computed tomography (CBCT)
Low-dose CBCT
Artificial intelligence (AI)
Dentofacial treatment

ABSTRACT

Objectives: Traditional cephalometric radiographs depict a three-dimensional structure in a two-dimensional plane; therefore, errors may occur during a quantitative assessment. Cone beam computed tomography, on the other hand, minimizes image distortion, allowing essential areas to be observed without overlap. Artificial intelligence can be used to enhance low-dose cone beam computed tomography images. This study aimed to clinically validate the use of artificial intelligence-processed low-dose cone beam computed tomography for generating two-dimensional lateral cephalometric radiographs by comparing these artificial intelligence-enhanced radiographs with traditional two-dimensional lateral cephalograms and those derived from standard cone beam computed tomography.

Methods: Sixteen participants who had previously undergone both cone beam computed tomography and plain radiography were selected. Group I included standard lateral cephalometric radiographs. Group II included cone beam computed tomography-produced lateral cephalometric radiographs, and Group III included artificial intelligence-processed low-dose cone beam computed tomography-produced lateral cephalometric radiographs. Lateral cephalometric radiographs of the three groups were analyzed using an artificial intelligence-based cephalometric analysis platform.

Results: A total of six angles and five lengths were measured for dentofacial diagnosis. There were no significant differences in measurements except for nasion-menton among the three groups.

Conclusions: Low-dose cone beam computed tomography could be an efficient method for cephalometric analyses in dentofacial treatment. Artificial intelligence-processed low-dose cone beam computed tomography imaging procedures have the potential in a wide range of dental applications. Further research is required to develop artificial intelligence technologies capable of producing acceptable and effective outcomes in various clinical situations.

* Corresponding author. Dentistry, Hallym University Sacred Heart Hospital, Gwanpyung-ro 170, Anyang, 14066, Republic of Korea.
E-mail address: purheit@hallym.or.kr (S.-H. Byun).

[1] Eun-Ji Chung and Byoung-Eun Yang contributed equally to this study.

https://doi.org/10.1016/j.heliyon.2024.e39445
Received 18 September 2023; Received in revised form 19 July 2024; Accepted 15 October 2024
Available online 4 November 2024

Clinical significance: Replacing standard cephalograms with cone beam computed tomography (CBCT) to evaluate the craniofacial relationship has the potential to significantly enhance the diagnosis and treatment of selected patients. The effectiveness of low-dose (LD)-CBCT was assessed in this study. The results indicated that lateral cephalograms reconstructed using LD-CBCT were comparable to standard lateral cephalograms.

1. Introduction

Since Hofrath and Broadbent introduced lateral cephalometric radiography in 1931, radiographs and cephalometric analysis have become standard tools for orthodontic evaluation and treatment planning [1–3]. When an exact evaluation is required, a standard cephalometric radiograph projects a three-dimensional (3D) object on a two-dimensional (2D) plane, which can result in discrepancies and differences among evaluations by different inspectors [4,5]. Additionally, based on radiation transmission, the midsagittal structures may have misleading shapes, which lower the accuracy of measurements in the overlapping structures [6].

Cone beam computed tomography (CBCT) is a high-resolution 3D imaging technique used in dentistry for various purposes, including implant surgery, orthodontic treatment planning, and root canal treatment. In the supine, standing, or sitting positions, CBCT scanners and the accompanying software have made it possible to quickly and effortlessly acquire and produce 3D multiplanar images [7–9].

Replacing standard cephalograms with CBCT for the evaluation of the craniofacial relationship has the potential to significantly advance the diagnosis and treatment of selected orthodontic and surgical patients [10]. Although CBCT is classified as a low-dose (LD) radiological technique, its effective radiation dose is higher than that of conventional dental radiography [11,12]. This is significant for pediatric use due to the greater danger of X-ray exposure in lower age groups. Indeed, radiologic examinations in dental-facial treatment are associated with a limited risk of radiation-induced diseases [13]. Since CBCT imaging has been proven to be a reliable method for dental-facial assessment, radiologic protocols can be limited to this one modality for initial diagnosis [14].

To avoid the risk of high-dose X-ray exposure in diagnosis, an LD-CBCT examination would be desirable [15]. However, reducing radiation dosage may have a negative impact on CBCT image quality by increasing noise and artifacts that can interfere with the diagnostic information in the resulting image [16]. Several techniques and optimization strategies have been used to improve LD-CBCT image quality [17]. The first method was designed to optimize the shooting parameters. Parameters such as the tube current, tube voltage, exposure time, and aperture can be adjusted to optimize the radiation dose. By lowering the tube current and voltage, shortening the exposure time, and limiting the scanning range, the radiation dose can be reduced while maintaining sufficient image quality [18–20]. The second method involved controlling the radiation dose. The tube current or exposure was adjusted using methods such as pulse limiting or real-time radiation dose control. By dynamically adjusting the radiation dose according to the absorption characteristics of the target, the radiation dose in the low-absorption area can be reduced, and the appropriate radiation dose in the high-absorption area can be maintained. Iterative reconstruction is the third strategy used to improve image quality. Iterative reconstruction methods with advanced features can enhance image quality while lowering radiation exposure. These algorithms utilize statistical modeling and iterative optimization techniques to compensate for radiation dose reduction by reconstructing high-quality images from limited projection data [11]. This study used the third method to investigate the efficacy of LD-CBCT.

Due to the rapid growth of deep learning technology, convolutional neural networks (CNN) have recently been used in multiple creative approaches to reduce the risks associated with the CBCT procedure. By harnessing the power of CNN, researchers and medical professionals address the concerns regarding radiation exposure in CBCT scans. One major advantage of CNN is their ability to automatically update relevant features from input data, leading to enhanced accuracy in image analysis. This facilitates the early detection of abnormalities, enabling timely and precise diagnosis of patients. Deep neural networks (DNN) are also widely used in CBCT applications. Their ability to process complex and high-dimensional data allows the modeling of intricate relationships within CBCT images [21–23]. This aids in segmentation tasks in which DNN can precisely delineate the anatomical regions of interest, which are essential for treatment planning and diagnosis [24,25]. Previous studies have achieved segmentation accuracy comparable to experienced radiologists by using extensive datasets [26,27]. Generative adversarial networks (GAN) are unique in their capacity to generate realistic synthetic images that closely resemble real CBCT scans. This has significant implications for data augmentation, where a limited dataset can be augmented with synthetic samples, thereby boosting the performance of CBCT models [28]. The integration of a recommended revolutionary trainable Sobel convolution marks a significant advancement in the capabilities of the edge-enhancement-based densely connected convolutional neural network (EDCNN). The synergy between the trainable Sobel convolution and EDCNN provides a powerful framework for edge enhancement in image processing and computer vision applications. Based on the module that used a trainable Sobel convolution, a densely connected model was built to combine the collected edge data and perform end-to-end image denoising. In this module, the learnable parameter α is defined in the learnable Sobel operator and is referred to as the Sobel factor, contrary to the typical fixed-value Sobel operator. Throughout the training process optimization, the value of this parameter could change, enabling the extraction of edge information in various intensities [29].

Despite the reduced radiation dose of CBCT, it would be of great clinical benefit if deep learning-based artificial intelligence (AI) technology could provide diagnostic results that are indistinguishable from those of standard cephalograms. Furthermore, obtaining detailed and diverse radiological images with a single CBCT scan and integrating existing conventional dentofacial diagnostic methods would be clinically advantageous.

This study aimed to clinically validate the use of AI-processed LD-CBCT for generating 2D lateral cephalometric radiographs by

comparing these AI-enhanced radiographs with traditional 2D lateral cephalograms and those derived from standard CBCT.

2. Results

Cephalometric radiographs and CBCT data were obtained from 16 participants, including 5 males and 11 females. The patients' ages ranged from 26 to 76 years, with an average age of 51.25 years. The lateral cephalograms used in this study are shown in Fig. 1. Table 1 indicates that all measurements were distributed within a 95 % confidence interval. No significant differences in variables except for nasion-menton (N-Me) (mm) were found. A significant difference was observed in N-Me (mm) ($F = 3.712$, $P < 0.05$). Post-hoc analysis of N-Me showed no significant differences between Groups II and III.

3. Discussion

This study demonstrates that 2D lateral cephalometric radiographs reconstructed from both standard CBCT and LD CBCT processed with AI are comparable to traditional 2D lateral cephalograms.

Differential values (N-Me) were found between the standard lateral cephalogram group (group I) and the CBCT groups (groups II and III). The reasons for this difference are the positioning of the patient when the radiograph is acquired and the difference in image acquisition methods between 2D standard lateral cephalography and 3D CBCT. In lateral cephalography, the film is positioned 15 cm from the midsagittal plane, and the X-ray source is fixed 5 feet away from it. In a CBCT machine, the radiation source moves around the patient, similar to how it is done in an orthopantogram. In addition, magnification was still observed in the lateral cephalography. These differences could cause magnification and distortion. Although this does not affect angle measurements between landmarks, absolute distances can be inconsistent between methodologies. Another reason for the observed difference was the use of landmarks for reconstruction. To convert from 3D CBCT to 2D cephalometric tomograms using the software, clinicians need to determine five points: both sides of the porions and orbitales, and one nasion. Once the clinician selects these five points, the 3D image is automatically converted into 2D. Despite the clinician's training, manually identifying cephalometric landmarks in the 2D plane has poor reproducibility, requires further training, and is potentially inaccurate.

The progress made in AI capabilities has had a profound impact on image analysis, particularly in medicine [30,31]. With the help of this advancement in AI, inexperienced clinicians can now properly identify and analyze landmark points in lateral cephalograms [32]. Measurement reproducibility is necessary to evaluate the accuracy of analytical methods. According to recent research, AI can recognize landmarks with equivalent accuracy to that of human examiners and may be a practical solution for the repetitive identification of numerous cephalometric landmarks [30,33,34]. The performance of an automated system has typically been compared

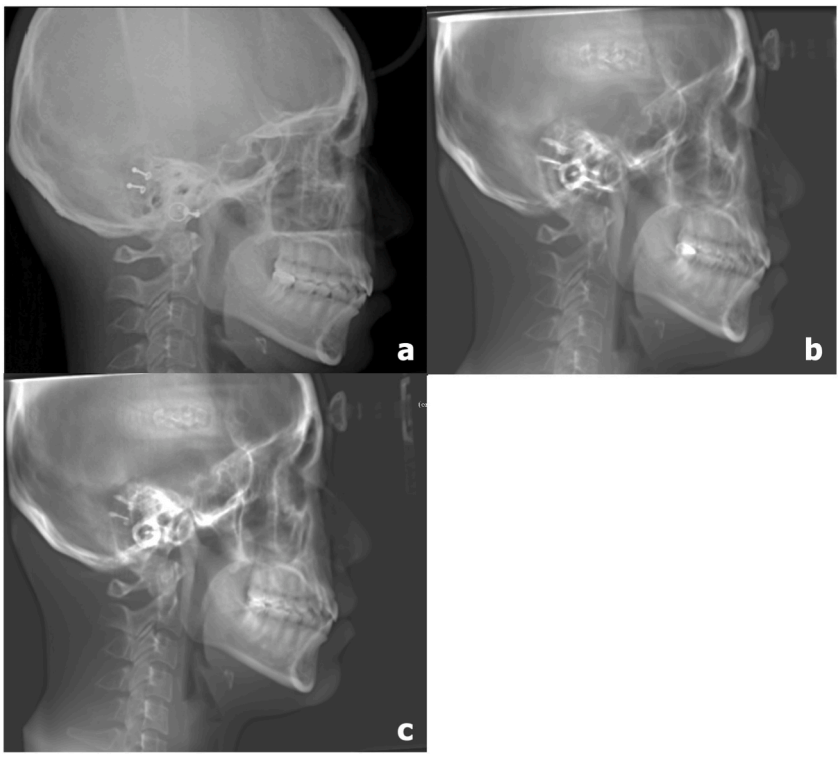

Fig. 1. Lateral cephalogram images used in this study. a) conventional lateral cephalogram; b) lateral cephalogram generated from CBCT; c) lateral cephalogram generated from AI-processed LD CBCT.

Table 1
Assessment of systematic bias between groups I, II, and III.

	Average	Standard Deviation	F	*p*
SNA (°)	83.88	4.82	1.969	0.151
	81.98	3.78		
	81.04	3.67		
SNB (°)	80.19	3.44	1.489	0.236
	78.69	2.96		
	78.43	2.92		
ANB (°)	3.68	2.06	1.454	0.244
	3.29	1.61		
	2.61	1.70		
SN-MP (°)	33.14	5.03	0.930	0.402
	35.18	5.02		
	35.28	4.95		
U1-MaxP (°)	112.48	6.02	0.185	0.831
	111.64	5.52		
	112.88	6.03		
L1-MP (°)	94.02	7.91	0.273	0.762
	92.78	6.82		
	92.15	7.09		
N-Me (°)	131.52	9.39[a]	3.712*	0.032
	139.84	9.99[b]		
	139.62	10.12[b]		
U1-NPog (mm)	9.68	2.43	0.024	0.976
	9.61	2.55		
	9.48	2.86		
L1-NPog (mm)	5.79	2.02	0.768	0.470
	4.81	2.71		
	4.96	2.45		
Upper Lip – E Line (mm)	−0.94	1.96	0.276	0.760
	−0.72	1.69		
	−0.46	1.79		
Lower Lip – E Line (mm)	0.34	2.51	0.006	0.994
	0.42	2.30		
	0.34	2.29		

*$P < 0.05$. Tukey's post-hoc analysis.

using the detection rates of skeletal landmarks within a 2-mm range, which has historically been acknowledged as a clinical error range in AI performance [35]. Therefore, an AI-based cephalometric analysis was implemented to increase the reliability of the study. To ensure the objectivity of cephalometric analysis, AI-based methods were used to compare and evaluate different images rather than relying on human assessment. Even when the same individual evaluates the same image, variations in results may occur depending on the circumstances. Thus, this study used AI-based cephalometric analysis to minimize such potential errors and ensure consistency in image evaluation.

LD-CBCT has emerged as a crucial trend in CBCT because of the potentially life-threatening risks associated with radiation exposure during routine CT scans [7]. Recently, deep learning-based approaches have emerged as potential solutions to overcome the computational complexity of previous mathematical algorithms for improving CBCT image quality [36]. Several deep learning algorithms have been developed for LD-CBCT. Various networks have been derived from U-shaped architectures (U-Nets), deep CNN, GANs, variational autoencoders (VAEs), and deep residual networks (ResNets). Several studies have found that the image quality of deep learning-based synthesized CT has improved overall, with considerably lower mean absolute error (MAE) differences compared with reference CT in both the testing and validation datasets [37]. Jiang et al. used a deep residual CNN to perform scatter correction on CBCT and claimed that it was computationally efficient [38]. Similarly, Li et al. demonstrated a better MAE after using an enhanced U-net design with a residual block and training the architecture on patients [36]. Yuan et al. used a similar approach in patients with head and neck cancer but with CBCT acquired at a fast-scan LD [39].

EDCNN was the deep learning algorithm used in the present study. With the aid of specialized learning technologies, it is developed with deep multilayer perception capable of creating a safe and improved classification model with nonlinear functions and linear, regularization, falling, and binary sigmoid classifications. As a result, deep learning prediction models and classification can help provide highly accurate and reliable evaluation while reducing the incidence of misdiagnosis [40]. This study found that LD-CBCT can provide images suitable for cephalometric analysis in dentofacial treatment. However, LD-CBCT may not be universally applicable to all clinical scenarios. The capability for cephalometric analysis does not imply the ability to diagnose every anatomical structure or pathological condition. In addition, cephalometric analysis is generally less affected by metal artifacts, as most landmarks and measurements used are not typically associated with metal restorations. Further advancements in these areas are essential if LD-CBCT is to effectively capture all necessary images for comprehensive dental treatment in a single session.

Through this study, LD-CBCT procedures could be advocated over conventional protocols because they provide acceptable image quality for diagnostic purposes while exposing patients to lower radiation doses in dentofacial treatment. However, further research is

needed to establish stronger evidence supporting LD-CBCT examinations as a viable alternative to traditional 2D methods in various clinical scenarios. In addition, compared to standard cephalography, LD-CBCT still uses a higher dose; therefore, the dose must be reduced further while being capable of producing an image of similar quality to that of the conventional image. Continued advancements in various AI processing technologies hold promise for improving the quality of CBCT images and dental treatment while simultaneously reducing the radiation dose associated with LD-CBCT.

4. Conclusions

The efficiency of LD-CBCT appears to be comparable to that of standard CBCT, and it has the advantage of being able to reconstruct various images. Because the quality of deep learning algorithms for LD-CBCT is subject to continuous improvement, more research is needed to optimize the image quality of LD-CBCT. Radiation exposure should be as low as diagnostically acceptable and should be indication-driven and patient-specific. More research is required to develop AI technologies capable of producing acceptable and effective results across various clinical situations.

5. Materials and methods

5.1. Study participants

The study included participants who had previously undergone both CBCT and plain radiography during their visit to the Hospital. CBCT was performed using bright MCT (Dentium, Suwon, South Korea). Patients with first molars and erupted incisors without maxillofacial abnormalities were included in the study. Among the 16 participants, the following three groups were created:

Group I consisted of standard cephalograms, whereas Group II included cephalometric radiographs regenerated using bright MCT (Dentium, Suwon, South Korea) and rainbow 3D Viewer (Dentium, Suwon, South Korea). Group III included cephalograms resynthesized by reducing the number of frames using AI processing. The study protocol was approved by the Institutional Review Board of Hospital (IRB No. 2021-07-016-005, 2021/09/14). Informed consent was obtained from all participants. The patients' private information was not disclosed. The radiographs were stored as TIFF files to facilitate comparison among the three groups.

Group I: Standard lateral cephalometric radiographs were obtained using RayScan Alpha (Ray Co., Gyeonggi-do, Korea). During imaging, the patients were placed in a cephalostat, and the head was stabilized by inserting ear rods of the head restraint into their ears. During imaging, the tube voltage ranged from 60 to 90 kV, the tube current from 4 to 17 mA, and the exposure time from 3.8 to 9.9 s.

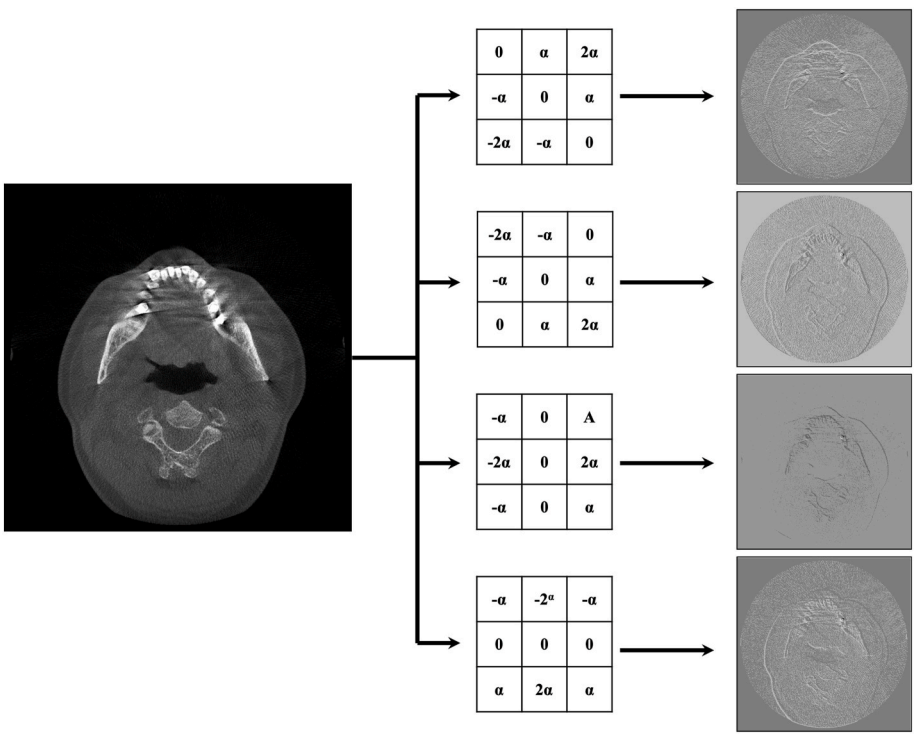

Fig. 2. The edge enhancement module. Four types of Sobel filters with a learnable parameter α.

Group II: bright MCT (Dentium, Suwon, South Korea) was used for the CBCT scans, with a field of view of 16 × 12 cm, slice thickness of 0.3 mm, 10 mA, 95 kV, and scan time of 20.16 s. The gathered data were imported into DICOM files.
Group III **(LD-CBCT):** bright MCT (Dentium, Suwon, South Korea) was used for the CBCT scans, with a field of view of 16 × 12 cm, slice thickness of 0.6 mm, 10 mA, 95 kV, and scan time of 20.16 s. The gathered data were AI-processed and imported into DICOM files.

5.2. AI processing from reducing the number of CBCT data

Within this study, operators were categorized into four distinct groups, encompassing vertical, horizontal, and diagonal orientations (Fig. 2). The parameter α was set to the value that minimizes the noise of the AI-processed CBCT, as illustrated in Fig. 2. This module encompasses multiple sets of trainable Sobel operators. The execution of this module (Fig. 3) began by running operations on the input CT image using a predetermined number (multiple of four) of trainable Sobel operators (EDCNN) to build a collection of feature maps to extract the edge information. The module then stacked the pictures in the channel dimensions with the input LD CT images to generate the final output. The number of 1x1 and 3x3 convolutional kernels was set uniformly to 32, with the exception of the last layer. The final 3x3 convolution layer consisted of a single kernel, corresponding to the output of a single channel. In Fig. 3, the green block comprises only two layers. However, the output of the edge enhancement module is connected to each of the seven green blocks through a skip connection. Through these dense connections, the extracted edge features can be fused and enhance the image.

The goal of this module was to improve the model's input information at the data-source level and increase the sensitivity of the model to edge information. Fig. 3 depicts the proposed network design, which creates an edge-improvement module using eight convolution blocks comprising the full model. The overall architecture of EDCNN consists of an edge enhancement module for extracting edge features, dense convolution blocks for feature fusion, and skip connections connecting the edge features to each dense block. Finally, the output is an image concatenating the fused edge features with the original image. The purpose of the model structure design after the edge-improvement module was to retain as many pictorial features as possible during the procedure. As demonstrated by the line in Fig. 3, this research transmitted the output of the edge-enhancement module to each convolutional block via a skip link, subsequently combining these outputs within the channel dimension. The voxel size of the CBCT image was 0.3 mm, and the volume consisted of 450 slices. This study used 270 cases for the training dataset and 30 cases for the test dataset, totaling approximately 120,000 images for model development. The test dataset was used independently.

5.3. Synthetization of lateral cephalometric radiographs from CBCT data

The saved DICOM and Communications in Medicine file from the CBCT was used to regenerate the 2D lateral cephalometric radiographs using rainbow 3D Viewer. The viewer generated lateral cephalometric radiographs by selecting the porion, orbitale, and nasion points. Fig. 4 shows the selection of the points.

5.4. Landmark identification and measurements

Lateral cephalometric radiographs were obtained in the three groups that were analyzed using AI-based WebCeph (Assemble

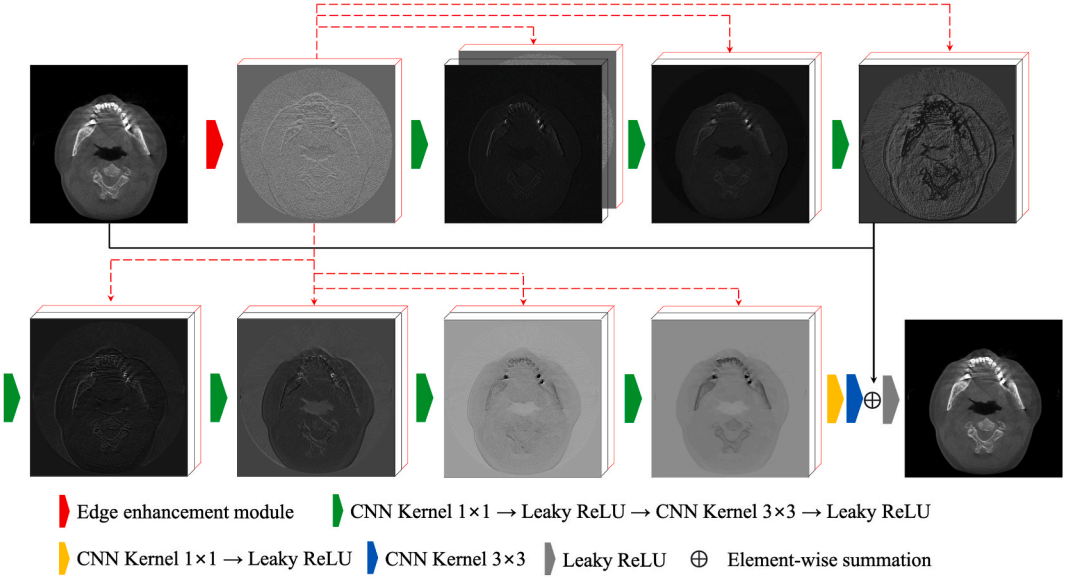

Fig. 3. The overall architecture of the AI model: EDCNN.

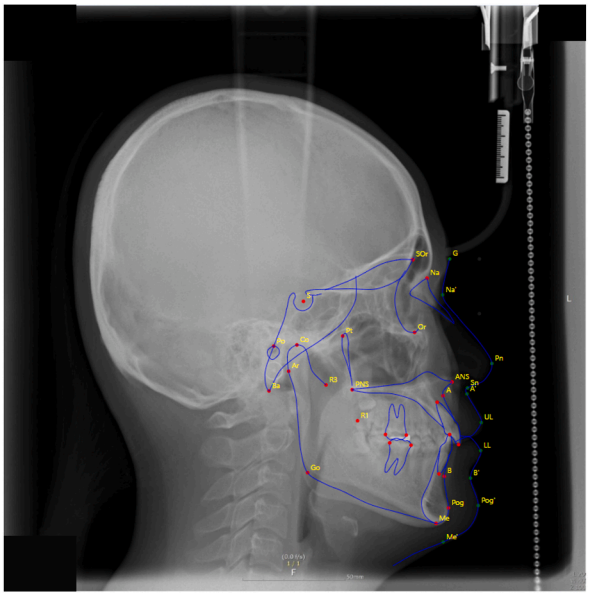

Fig. 4. AI-based cephalometric tracing.

Circle, Gyeonggi-do, Korea) [41]. The automated tracing of measurement sites on WebCeph is shown in Fig. 5 [15]. Each lateral cephalometric radiograph had 17 measurement points and 11 measurements reflecting skeletal, dental, and soft tissue features, including SNA (sella-nasion-point A), SNB (sella-nasion-point B), ANB (point A-nasion-point B), SN-MP (sella nasion-mandibular plane), U1-MaxP (upper 1-maxillary plane), L1-MP (lower 1-mandibular plane), N-Me (nasion-menton), U1-NPog (upper 1-nasion pogonion), L1-NPog (lower 1-nasion pogonion), upper lip-E line (upper lip-esthetic line), and lower lip-E line (lower lip-esthetic line) measurements. A single measurement point was created by averaging the bilateral structures [12].

5.5. Statistical analysis

The Statistical Package for the Social Sciences for Windows (version 27.0; SPSS Inc., Chicago, Illinois, USA) was used for all statistical analyses. The presentation of the data includes the mean, standard deviation, standard error, and significance values. One-way analysis of variance and Tukey's post-hoc test were used to compare how the measured values varied among the three groups. A 95 % confidence range was used to evaluate the research group's findings, and $P < 0.05$ was regarded as statistically significant.

CRediT authorship contribution statement

Eun-Ji Chung: Writing – review & editing, Writing – original draft, Resources, Methodology, Investigation, Data curation. **Byoung-Eun Yang:** Supervision, Software, Project administration, Funding acquisition, Conceptualization. **Sam-Hee Kang:** Visualization, Validation. **Young-Hee Kim:** Visualization, Supervision, Software. **Ji-Yeon Na:** Investigation, Data curation. **Sang-Yoon Park:** Software, Project administration, Formal analysis, Data curation. **Sung-Woon On:** Supervision, Project administration, Methodology. **Soo-Hwan Byun:** Writing – review & editing, Writing – original draft, Validation, Supervision, Software, Resources, Project administration, Funding acquisition, Data curation, Conceptualization.

Availability of data and materials

The datasets supporting the conclusions of this study are included in this article. The datasets used and/or analyzed in the current study are available from the corresponding author upon reasonable request.

Ethics approval and consent to participate

The study was conducted in accordance with the guidelines of the Declaration of Helsinki and was approved by the Institutional Review Board of Hallym University Sacred Heart Hospital (IRB approval No. 2021-07-016-005, 2021/09/14). The personal information of the patients was not disclosed throughout the study or publication process.

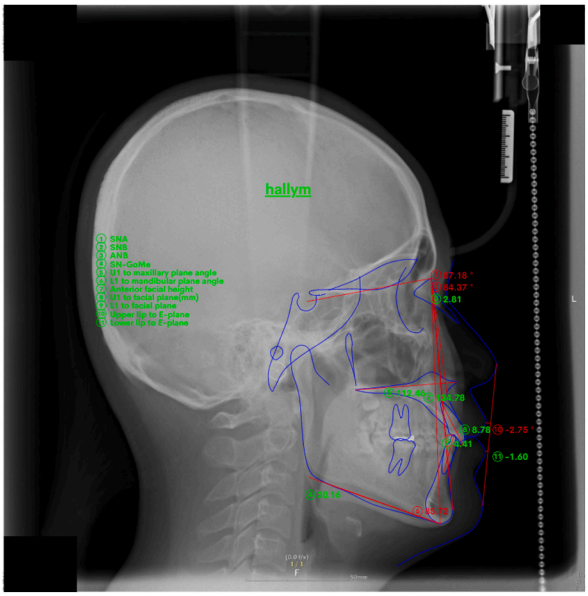

Fig. 5. AI-based cephalometric analysis.

Consent for publication

Written informed consent for the publication of potentially identifiable information was obtained from all participants.

Funding

This work was supported by National IT Industry Promotion Agency (NIPA) grant funded by the Korean government (MSIT) (S1402-23-1001, AI Diagnostic Assisted Virtual Surgery and Digital Surgical Guide for Dental Implant Treatment in the Post-Aged Society: A Multicenter Clinical Demonstration).

This work was supported by the Nano-Convergence Foundation (www.nanotech2020.org) funded by the Ministry of Science and ICT (MSIT, Korea) & the Ministry of Trade, Industry and Energy (MOTIE, Korea) [Project Name: Dental implant placement guide robot system based on permanent magnet positioning device/ Project Number: 20014921].

This work was supported by the Korea Medical Device Development Fund grant funded by the Korea government (the Ministry of Science and ICT, the Ministry of Trade, Industry and Energy, the Ministry of Health & Welfare, the Ministry of Food and Drug Safety) (Project Number: KMDF001409351G0003232).

Declaration of competing interest

The authors declare that they have no known competing financial interests or personal relationships that could have appeared to influence the work reported in this paper.

Acknowledgements

Not applicable.

References

[1] S.F. Albarakati, K.S. Kula, A.A. Ghoneima, The reliability and reproducibility of cephalometric measurements: a comparison of conventional and digital methods, Dentomaxillofacial Radiol. 41 (1) (2012) 11–17.
[2] P.G. Nijkamp, et al., The influence of cephalometrics on orthodontic treatment planning, Eur. J. Orthod. 30 (6) (2008) 630–635.
[3] A. Omran, et al., Mandibular shape prediction using cephalometric analysis: applications in craniofacial analysis, forensic anthropology and archaeological reconstruction, Maxillofac Plast Reconstr Surg 42 (1) (2020) 37.
[4] M.O. Lagravere, et al., Intraexaminer and interexaminer reliabilities of landmark identification on digitized lateral cephalograms and formatted 3-dimensional cone-beam computerized tomography images, Am. J. Orthod. Dentofacial Orthop. 137 (5) (2010) 598–604.
[5] J.W. Choi, et al., Positional symmetry of porion and external auditory meatus in facial asymmetry, Maxillofac Plast Reconstr Surg 37 (1) (2015) 33.
[6] S.Y. Park, et al., Comparison of time and cost between conventional surgical planning and virtual surgical planning in orthognathic surgery in Korea, Maxillofac Plast Reconstr Surg 43 (1) (2021) 18.
[7] A.W. Yeung, R. Jacobs, M.M. Bornstein, Novel low-dose protocols using cone beam computed tomography in dental medicine: a review focusing on indications, limitations, and future possibilities, Clin. Oral Invest. 23 (2019) 2573–2581.

[8] D.S. Hwang, J.S. Seo, H.S. Choi, Skeletal stability after 2-jaw surgery via surgery-first approach in facial asymmetry patients using CBCT, Maxillofac Plast Reconstr Surg 42 (1) (2020) 11.
[9] S.H. Kim, S.K. Choi, Changes in the hyoid bone, tongue, and oropharyngeal airway space after mandibular setback surgery evaluated by cone-beam computed tomography, Maxillofac Plast Reconstr Surg 42 (1) (2020) 27.
[10] H.L. Cao, et al., Quantification of three-dimensional facial asymmetry for diagnosis and postoperative evaluation of orthognathic surgery, Maxillofac Plast Reconstr Surg 42 (1) (2020) 17.
[11] Z. Hu, et al., Artifact correction in low-dose dental CT imaging using Wasserstein generative adversarial networks, Med. Phys. 46 (4) (2019) 1686–1696.
[12] D.A. Pierce, D.L. Preston, Radiation-related cancer risks at low doses among atomic bomb survivors, Radiat. Res. 154 (2) (2000) 178–186.
[13] J. Ver Berne, et al., Cumulative exposure and lifetime cancer risk from diagnostic radiation in patients undergoing orthognathic surgery: a cross-sectional analysis, Int. J. Oral Maxillofac. Surg. (2023).
[14] P. Pittayapat, et al., Agreement between cone beam computed tomography images and panoramic radiographs for initial orthodontic evaluation, Oral Surg Oral Med Oral Pathol Oral Radiol 117 (1) (2014) 111–119.
[15] E.J. Chung, et al., Effectiveness of cone-beam computed tomography-generated cephalograms using artificial intelligence cephalometric analysis, Sci. Rep. 12 (1) (2022) 20585.
[16] C. Jiang, et al., Geometric calibration of a stationary digital breast tomosynthesis system based on distributed carbon nanotube X-ray source arrays, PLoS One 12 (11) (2017) e0188367.
[17] F.S. Schwindling, et al., In vitro diagnostic accuracy of low-dose CBCT for evaluation of peri-implant bone lesions, Clin. Oral Implants Res. 30 (12) (2019) 1200–1208.
[18] D. Jones, et al., The effect of alteration of the exposure parameters of a cone-beam computed tomographic scan on the diagnosis of simulated horizontal root fractures, J. Endod. 41 (4) (2015) 520–525.
[19] R. Goulston, et al., Dose optimization by altering the operating potential and tube current exposure time product in dental cone beam CT: a systematic review, Dentomaxillofacial Radiol. 45 (3) (2016) 20150254.
[20] A.-M. Ilo, et al., Minimum size and positioning of imaging field for CBCT-scans of impacted lower third molars: a retrospective study, BMC Oral Health 21 (2021) 1–10.
[21] H. Chen, et al., Low-dose CT with a residual encoder-decoder convolutional neural network, IEEE Trans Med Imaging 36 (12) (2017) 2524–2535.
[22] Y. Fu, et al., Deep learning in medical image registration: a review, Phys. Med. Biol. 65 (20) (2020) 20TR01.
[23] T. Li, et al., Motion correction of respiratory-gated PET images using deep learning based image registration framework, Phys. Med. Biol. 65 (15) (2020) 155003.
[24] S. Kida, et al., Cone beam computed tomography image quality improvement using a deep convolutional neural network, Cureus 10 (4) (2018) e2548.
[25] N. Yuan, et al., Convolutional neural network enhancement of fast-scan low-dose cone-beam CT images for head and neck radiotherapy, Phys. Med. Biol. 65 (3) (2020) 035003.
[26] Z. Cui, et al., A fully automatic AI system for tooth and alveolar bone segmentation from cone-beam CT images, Nat. Commun. 13 (1) (2022) 2096.
[27] D. Kainmueller, et al., Automatic extraction of mandibular nerve and bone from cone-beam CT data, Med Image Comput Comput Assist Interv 12 (Pt 2) (2009) 76–83.
[28] N. Yuan, et al., Head and neck synthetic CT generated from ultra-low-dose cone-beam CT following Image Gently Protocol using deep neural network, Med. Phys. 49 (5) (2022) 3263–3277.
[29] T. Liang, et al., Edcnn: edge enhancement-based densely connected network with compound loss for low-dose ct denoising, in: 2020 15th IEEE International Conference on Signal Processing (ICSP), IEEE, 2020.
[30] H.W. Hwang, et al., Evaluation of automated cephalometric analysis based on the latest deep learning method, Angle Orthod. 91 (3) (2021) 329–335.
[31] R. Rokhshad, S.O. Keyhan, P. Yousefi, Artificial intelligence applications and ethical challenges in oral and maxillo-facial cosmetic surgery: a narrative review, Maxillofac Plast Reconstr Surg 45 (1) (2023) 14.
[32] C. Lindner, et al., Fully automatic system for accurate localisation and analysis of cephalometric landmarks in lateral cephalograms, Sci. Rep. 6 (1) (2016) 33581.
[33] A.K. Subramanian, et al., Cephalometric analysis in orthodontics using artificial intelligence—a comprehensive review, BioMed Res. Int. (2022) 2022.
[34] G. Bulatova, et al., Assessment of automatic cephalometric landmark identification using artificial intelligence, Orthod. Craniofac. Res. 24 (2021) 37–42.
[35] W. Geelen, et al., Reproducibility of cephalometric landmarks on conventional film, hardcopy, and monitor-displayed images obtained by the storage phosphor technique, Eur. J. Orthod. 20 (3) (1998) 331–340.
[36] Y. Jiang, et al., Scatter correction of cone-beam CT using a deep residual convolution neural network (DRCNN), Phys. Med. Biol. 64 (14) (2019) 145003.
[37] Y. Zhang, et al., Improving CBCT quality to CT level using deep learning with generative adversarial network, Med. Phys. 48 (6) (2021) 2816–2826.
[38] P. Isola, et al., Image-to-image translation with conditional adversarial networks, in: Proceedings of the IEEE Conference on Computer Vision and Pattern Recognition, 2017.
[39] N. Yuan, et al., Convolutional neural network enhancement of fast-scan low-dose cone-beam CT images for head and neck radiotherapy, Phys. Med. Biol. 65 (3) (2020) 035003.
[40] B. Qiu, et al., Recurrent convolutional neural networks for 3D mandible segmentation in computed tomography, J. Personalized Med. 11 (6) (2021) 492.
[41] R.K. Mahto, et al., Evaluation of fully automated cephalometric measurements obtained from web-based artificial intelligence driven platform, BMC Oral Health 22 (1) (2022) 132.